ORGANOMETALLICS

Article

pubs.acs.org/Organometallics

Ammonium Arylspiroborate Compounds: Synthesis, Crystal Structure, Fluorescence Properties, and Antibacterial Activity

Qiaoyun Wang and Hong Zhou*

School of Chemistry and Environmental Engineering, Wuhan Institute of Technology, 693 Xiongchu Avenue, Wuhan 430073, People's Republic of China

Supporting Information

ABSTRACT: A series of R-substituted ammonium arylspiroborate compounds (R = CH_3, H, F, Cl, Br) have been synthesized via a facile one-pot method. The structures of these new kinds of boron compounds were characterized by IR, NMR spectra, elemental analysis and X-ray diffraction techniques, and their possible formation mechanism was proposed. Surprisingly, the as-synthesized boron compounds showed multifunctional character with not only excellent fluorescence properties (high quantum yields and large Stokes shift) in both the liquid and solid state but also high antibacterial activity against both Gram-negative (*E. coli*) and Gram-positive (*S. aureus*) bacteria. The chlorine-substituted boron compound even possessed antibacterial activity comparable with that of commercial antibiotics. More importantly, the fluorescence properties and antibacterial activity of these boron compounds could be easily mediated by the variation of the substituents, which was proved to regulate the conjugated system, modify the hydrophobic character, and adjust the electric charge on the surface of boron compounds. In addition, the influence of different factors including solvent (i.e., polarity, concentration), temperature, and pH on the fluorescence properties of boron compounds was discussed in detail. This work provides a new strategy for the design of multifunctional organoboron compounds and the mediation of their properties.

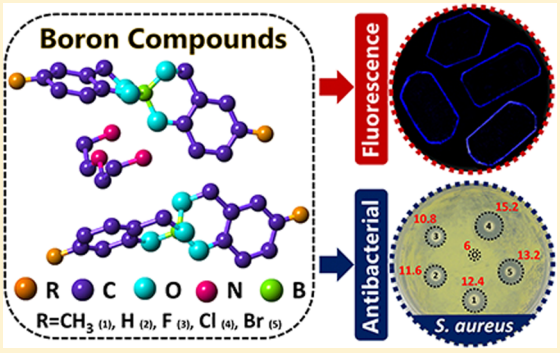

1. INTRODUCTION

Luminescent complexes have attracted significant attention owing to their potential applications in organic light-emitting diodes (OLEDs), solar cells, laser dyes, photosensitizers, biomolecular labels, and molecular probes.[1−11] Most fluorescent materials are highly fluorescent in dilute solution but weakly luminescent or even nonemissive in the solid state, a phenomenon known as aggregation-caused quenching (ACQ).[12−15] One factor is that these materials pack tightly in the amorphous solid phase or crystalline state, and another main factor is the energy loss via rotational movements, which results in significant self-quenching of the emission and restricts their potential application. As far as we know, fluorescent organic solids are highly sought for applications in many advanced technologies, including chemical sensing, bioimaging, information display, and organic photonics.[16−20] Therefore, it is meaningful to develop new kinds of fluorescent materials which can emit strong fluorescence with high quantum efficiency not only in the liquid form but also in the solid state.

Organoboron compounds are one of the most important types of fluorescent materials, which have attracted much attention due to their excellent optical properties with sharp absorption bands, high fluorescence quantum yields, high molar extinction coefficients, and chemical stability.[21−26] In recent years, boron diketonate derivatives have emerged as excellent fluorescent materials for their promising luminescent properties with high quantum yields and large Stokes shifts not only in the liquid form but also in the solid state.[27−30] However, the types of luminescent organoboron compounds with high efficiency are still limited and the discussion about different influencing factors on their fluorescence properties is not systematic at present, which hinders their development and practical application in high-tech industry.

On the other hand, boron has been acknowledged as a trace element with the characteristics of low mammalian toxicity, high activity, nonflammability, and noncorrosiveness, which contribute to the significant importance of boron compounds in a series of biochemical applications such as protecting groups,[31,32] enzyme inhibitors, biosensors,[33,34] neutron capturing agents for cancer therapy,[35] bioconjugates, and protein labels. Among various natural and synthetic boron compounds, some have been proved to exhibit antibacterial, antifungal, antimalarial, and antiviral activities.[36,37] For example, it has recently been reported that an organo-soluble borate ester compound with tetrahedral ammonium as the countercation showed obvious biological activity against wood decay fungi.[38−40] In addition, one boron compound (sodium boranocarbonate) has been reported as the first water-soluble and non-transition-metal-containing CO-releasing molecule

Received: June 13, 2017

DOI: 10.1021/acs.organomet.7b00435
Organometallics XXXX, XXX, XXX−XXX

(CO-RM); its biological properties has also been thoroughly investigated.[41] All these facts indicate that boron compounds can be considered as potential agents for antibacterial, antimalarial, and antiviral applications.

Due to the attraction of the many advantages of boron compounds, a series of R-substituted ammonium arylspiroborate compounds (R = CH_3, H, F, Cl, Br) have been designed and synthesized via a facile one-pot method. The structures of these new kinds of boron compounds were characterized by IR, NMR spectra, elemental analysis, and X-ray diffraction techniques, and their possible formation mechanism was proposed. Surprisingly, the as-synthesized boron compounds showed multifunctional character with not only excellent fluorescence properties (high quantum yields and large Stokes shift) in both the liquid and solid state but also high antibacterial activity against both Gram-negative (*E. coli*) and Gram-positive (*S. aureus*) bacteria. The chlorine-substituted boron compound even possessed antibacterial activity comparable to that of commercial antibiotics. More importantly, the fluorescence properties and antibacterial activity of these boron compounds could be easily mediated by the variation of the substituents, which was proved to regulate the conjugated system, modify the hydrophobic character, and adjust the electric charge on the surface of boron compounds. In addition, the influence of different factors including solvent (i.e., polarity, concentration), temperature, and pH on the fluorescence properties of boron compounds was examined systematically. The methyl-substituted boron compound exhibited the best fluorescence properties in all cases. This work provides a new strategy for the design of multifunctional organoboron compounds and the mediation of their properties.

2. EXPERIMENTAL SECTION

2.1. Materials. The various aldehydes, dimethyl sulfate, benzotriazole, BH_3·THF, and ciprofloxacin were purchased from Aladdin (Shanghai, China). 1,2-Dichloroethane (DCE), sodium hydroxide, hydrochloric acid, diethylenetriamine (DETA), cyclohexane (CYH), toluene (TL), tetrahydrofuran (THF), acetonitrile (AN), and methyl alcohol (MeOH) were obtained from Sinopharm Chemical Reagent Co. (China). The strains of *S. aureus*, *B. subtilis*, *E. coli* and *P. aeruginosa* were purchased from Southern Biological. All reagents were analytical grade and were used as received.

2.2. Synthesis. *2.2.1. Synthesis of 1-Methylbenzotriazole−Borane (MeBtb).* 1-Methylbenzotriazole was synthesized according to a previously reported method with some modifications[27] (Scheme 1). First, benzotriazole (40.810 g, 342.50 mmol) was dissolved in sodium hydroxide solution (14.00 mol/L). Then dimethyl sulfate (48.020 g, 380.70 mmol) was dropped into the above solution with vigorous stirring for 2.5 h at room temperature. After that, the mixture was washed with 2 N hydrochloric acid until the pH reached 3 and then cooled in an ice−water bath. 1-Methylbenzotriazole (MeBt) was obtained after the precipitate was filtered, washed with 1.00 mol/L sodium hydroxide (3 × 10.00 mL), and dried at room temperature (29.402 g, yield 65%) Mp: 61−62 °C (lit.[42] mp 65 °C). Anal. Calcd for $C_7H_7N_3$: H, 5.51; C, 63.08; N, 31.38. Found: H, 5.30; C, 63.14; N, 31.56. ^{1}H NMR (d_6-DMSO): δ 4.30 (s, 3H), 7.37−7.41 (m, 1H), 7.52−7.56 (m, 1H), 7.81−7.84 (m, 1H), 8.01−8.03 (m, 1H).

Scheme 1. Synthesis of 1-Methylbenzotriazole−Borane (MeBtb)

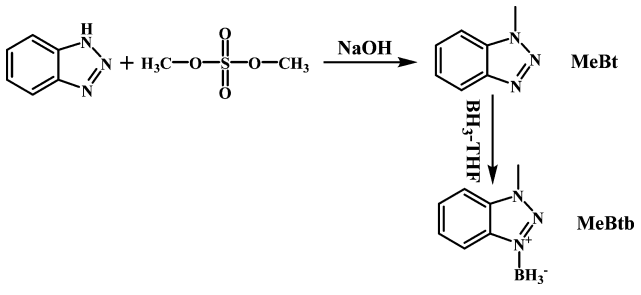

To synthesize MeBtb, the obtained MeBt (1.331 g, 10.00 mmol) was dissolved in dried THF (10.00 mL) in a 50.00 mL round-bottom flask. Then BH_3·THF (11.00 mL) was added dropwise by a syringe with continuous stirring in an ice−water bath for 2 h. After the completion of the reaction, MeBtb (1.233 g, yield: 84%) was obtained by filtration as a white solid. Mp:187−188 °C (lit.[43] mp 187.2−188.9 °C). Anal. Calcd for $C_7H_{10}BN_3$: H, 6.66; C, 57.39; N, 28.46. Found: H, 6.88; C, 57.20; N, 28.59. ^{1}H NMR (300 MHz, $CDCl_3$): δ 8.17−8.15 (m, 1H), 7.68−7.64 (m, 2H), 7.63−7.58 (m, 1H), 4.37 (s, 3H), 2.73−2.54 (br m, 3H).

2.2.2. Synthesis of Boron Compounds. Compound **1** was prepared as follows (Scheme 2): 5-methylsalicylaldehyde (1.365 g, 10.00 mmol)

Scheme 2. Synthesis of Boron Compounds

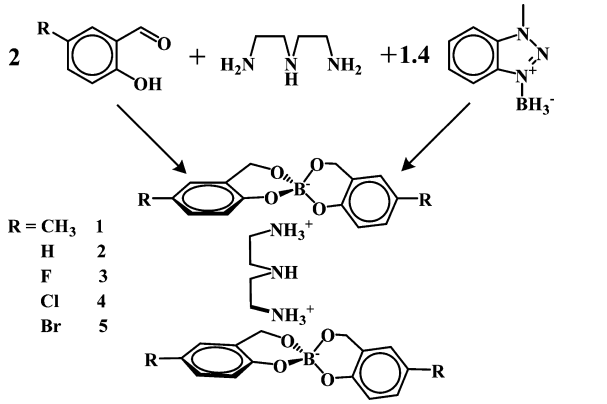

was dissolved in 20.00 mL of DCE. Then *N*-1-methyl-3-boranebenzotriazole (1.023 g, 7.00 mmol) was added to this mixture with stirring for 30 min to form a clear solution. After that, diethylenetriamine (0.515 g, 5.00 mmol) was dropped into this solution, followed by stirring for 6 h at room temperature. The mixture was then filtered and wished with DCE (3 × 10.00 mL). The final products were obtained by crystallization in ethanol to form flaky crystals (2.094 g, yield 97%). ^{1}H NMR (400 MHz, CD-DMSO): δ 6.74−6.72 (m, 1H), 6.61(d, 1H), 6.37 (d, 1H), 4.54 (s, 2H), 2.74 (t, 1H), 2.58 (t, 1H), 2.15 (s, 3H). ^{13}C NMR (100 MHz, CD-DMSO): δ 155.3, 127.6, 126.3, 125.2, 124.4, 116.7, 60.7, 20.8. Anal. Calcd for **1**, $C_{36}H_{45}B_2N_3O_8$: H, 6.56; C, 64.61; N, 6.34. Found: H, 6.78; C, 64.59; N, 6.28. Mp: 223−224 °C. IR (cm^{-1}, KBr disk): 2920 m, 2833 w, 1619 w, 1499 s, 1456 m, 1359 w, 1275 s, 1232 w, 1128 s, 1091 m, 1039 m, 941 m, 876 m, 820 w, 764 s.

The other four compounds (**2**−**5**) were synthesized in the same way as for compound **1** except that 5-methylsalicylaldehyde was replaced by salicylaldehyde, 5-fluorosalicylaldehyde, 5-chlorosalicylaldehyde, and 5-bromosalicylaldehyde, respectively. The other synthetic steps were totally identical. The yields of compounds **2**−**5** were 99%, 93%, 95%, and 95%, respectively, and the melting points were 221−222, 234−235, 232−233, and 229−230 °C for compounds **2**−**5**, respectively. The other characterization data for compounds **2**−**5** can be found in the Supporting Information.

Crystals of boron compounds **1**−**5** suitable for X-ray analysis were obtained by slow diffusion of diethyl ether into a saturated methanol solution of the as-prepared compounds for several weeks.

2.3. Characterization. The FT-IR spectra were measured on a Nicolet Magna 750 FT-IR spectrometer in the range of 4000−400 cm^{-1} by using KBr pellets. Elemental analyses were recorded with a PerkinElmer 240 analyzer. ^{1}H NMR spectra were measured on Bruker 400 MHz and Varian 300 M instruments for solutions in $CDCl_3$ and

DOI: 10.1021/acs.organomet.7b00435
Organometallics XXXX, XXX, XXX−XXX

CD-DMSO. ^{13}C NMR spectra were recorded on a Bruker 100 MHz instrument with complete proton decoupling for solutions in CD-DMSO. Chemical shifts are reported in ppm from tetramethylsilane with the solvent resonance as internal standard. The absorption spectra were recorded on a PerkinElmer Lambda 35 UV/vis spectrophotometer at room temperature. The emission spectra were recorded on a PerkinElmer LS55 spectrofluorimeter equipped with a commercial low-temperature accessory and a special commercial cuvette. The fluorescence spectra in the solid phase were measured from the surface of the pressed powder in the special cuvette. The spectra were corrected for the characteristics of the emission monochromator and for the photomultiplier response and by excitation at a wavelength of 370 nm. The fluorescence spectra in the liquid phase were measured at room temperature. The static contact angles (CAs) were recorded by a Dataphysics OCA 20 (Germany) contact angle measuring instrument, using 3 μL of a water or oil droplet at ambient temperature. The fluorescence images were acquired with an inverted fluorescence microscope (Leica DMIL) equipped with a Nikon digital camera. A 360 nm laser was used to excite the samples during imaging.

2.4. Crystallography. The X-ray single-crystal diffraction measurements of the obtained boron compounds were performed in sequence on a Super Nova, Dual, Cu at zero, Atlas diffractometer. Crystallographic data and structure refinement data were obtained by using the SMART and SAINT programs. All structures were solved by direct methods using SHELXS-2014 and refined on F^2 by full-matrix least squares (SHELXS-2014) in the WINGX environment. The non-H atoms were treated as anisotropic. The H atoms were placed in calculated positions and refined isotropically using the riding mode.

2.5. Antibacterial Activities of Compounds. To evaluate the antibacterial activities of the as-prepared boron compounds, inhibition zone, inhibition curves, colony counting and leakage of reducing sugars were preformed against Gram-positive *S. aureus* and *B. subtilis* and Gram-negative *E. coli* and *P. aeruginosa*. The quantity of the bacteria and the sample used in the antibacterial test are given in Table 1.

Table 1. Quantity of the Bacteria and the Sample Used in the Antibacterial Test

		antibacterial activity of boron compounds			
		inhibition zone test	growth inhibition curve	colony counting test	reducing sugars
bacteria[a]	V (μL)	20	20	2×10^3	10^4
	C (CFU/mL)	10^8	10^8	10^5	10^8
sample	V (μL)	10	20	2×10^3	10^4
	C (μg/mL)	5	*b*	*b*	10^2

[a]Bacterium: incubation in the LB liquid medium at 37 °C for 24 h with an initial concentration of 10^8 CFU/mL (optical density 0.068−0.075 at 660 nm). [b]Sample with a different concentration.

3. RESULTS AND DISCUSSION

3.1. Structural Descriptions. The five boron compounds obtained were characterized by IR spectra (Figure S13 in the Supporting Information) and X-ray technology, and their crystallographic data and details about the data collection and refinement are summarized in Table S1 in the Supporting Information. Figure 1a shows the molecular structure of compound **2**, which crystallized in the monoclinic phase with space group $C1_2$ and is composed of two anionic boron coordination structure units and one ammonium countercation (diethylenetriamine with two primary amine protonations). Each of the two borate anions consists of two deprotonated 2-(hydroxymethyl)-4-R-phenol (L) and one B^{3+} ion, where B^{3+} covalently connects two phenoxide and two hydroxymethyl groups (from L), resulting in tetrahedral coordination. The B−O bond lengths in compound **2** are in the range of 1.42−1.52 Å, which are typical for such tetrahedral borates and consistent with the values in the Cambridge Structural Database (CSD).[44] In the boron tetrahedral configuration, the angles of boron atoms bonded with two oxide atoms from the same L (i.e., angles between planes C and D and planes C′ and D′) are almost vertical (87.28 and 89.88°) but are slightly different, leading to a slightly distorted tetrahedral configuration (Table S3 in the Supporting Information). The protonated diethylenetriamine cation in compound **2** serves mainly as a charging balance counterpart and is located in the middle of the two boron structure units with B1−N1 and B2−N1 distances of 3.737(4) and 5.707(4) Å, respectively.

There are abundant hydrogen bonds in the obtained boron compounds. Here we use compound **2** as an example. As shown in the hydrogen bond topology diagrams of compound **2** (Figure 1b), the protonated diethylenetriamine cation is located in the middle of the two anions, acting as a hydrogen bond donor that connects two anionic boron coordination structure units through seven N−H···O interactions. The N···O distances are in the range of 2.220−3.244 Å, and the N−H···O angles are in the range 116.6−169.4°. Two anionic boron coordination structure units connect with each other through C(7)−H(7B)···O(5) hydrogen bond interactions with C···O distances of 3.438 Å. Every chain in compound **2** connects with two adjacent chains through the two hydrogen bond interactions N(2)−H(2A)···O(4) and N(3)−H(3C)···O(6). Furthermore, the hydrogen bond interactions through N(2)−H(2C)···O(8) lead to the construction of the 2D network.

The molecular structures and hydrogen bond topology diagrams of the other four boron compounds are shown in Figure S14a−d and Figure S14e−h in the Supporting Information, respectively. Obviously, other than the difference in substituents in the benzene groups, the other four boron compounds possess molecular structures similar to that of compound **2**. In addition, their hydrogen bonds are basically the same as those of compound **2**, except for slight variations in the lengths and angles of the bonds, which lead to slight differences in the three-dimensional network (the hydrogen bond data are given in Table S5 in the Supporting Information).

3.2. Possible Formation Mechanism. As described in Scheme 3, the reaction is initiated from the reduction of triazole−boranes caused by salicylic aldehyde derivatives with different substituents (CH_3, H, F, Cl, and Br), which involves hydride ion transfer from the triazole−boranes to the carbonyl carbon of salicylic aldehyde derivatives to form O^- and BH_2. Then the unsaturated boron in BH_2 binds with oxygen atoms to become negatively charged and thus form the octet structure, which undergoes a hydrolysis process afterward to generate a secondary alcohol and boric acid (step 1).[45−47] After that, the presence of DETA can trigger dehydrogenation at phenolic *p*-hydroxy groups of alicylic alcohol derivatives. As illustrated in step 2, the deprotonated phenolic hydroxy groups can not only condense with the hydroxy group of the boric acid but also nucleophilically attack the empty orbital of boric acid, so that boric acid can form the 1:1 monochelate first and then eventually form 1:2 bidentate complexes with the corresponding salicyl alcohol derivatives.[48] Specifically, the procedure of this reaction can be divided into the following: first, boric acid,

DOI: 10.1021/acs.organomet.7b00435
Organometallics XXXX, XXX, XXX−XXX

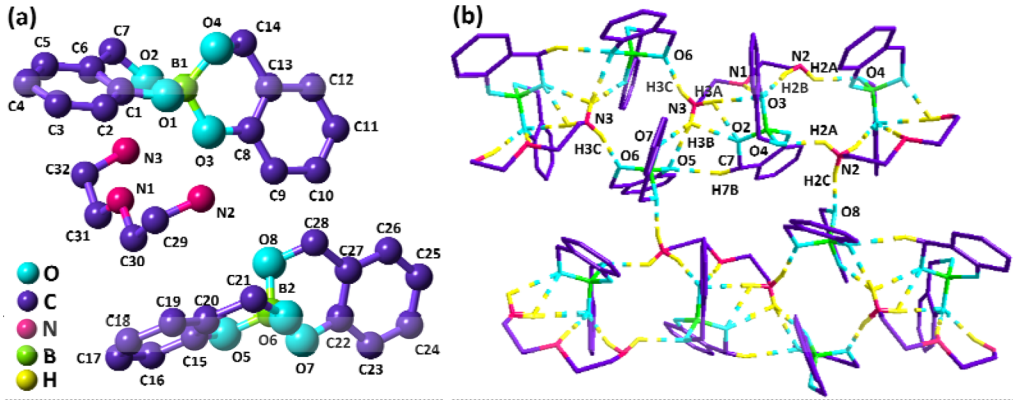

Figure 1. (a) Molecular structure of compound **2** with atom labels (the other four compounds have the same atom labels with compound **2** except for different substituents at C4, C11, C17, and C25). Hydrogen atoms have been omitted for clarity. (b) Hydrogen bond topology diagrams of compound **2**. The hydrogen atoms and solvent molecules which are not involved in hydrogen bond interactions are omitted for clarity.

which is one product in the first step, would accept an electron pair through the nucleophilic attack of the deprotonated phenolic hydroxy groups, followed by a condensation reaction with the alcoholic hydroxy group of the ligand to form the 1:1 monochelate complex; then it reacts with the protonated salicyl alcohol moieties. This condensation reaction results in the generation of a 1:2 bis-chelate complex and two water molecules. Because one DETA can deprotonate two hydroxy groups, there are two anionic boron coordination compounds and a protonated DETA countercation with a positive charge of +2 in the final product.

3.3. Fluorescence Properties. The absorption and fluorescence emission spectra of as-prepared boron compounds **1**−**5** were recorded in MeOH with a concentration of 1×10^{-4} mol/L, and the relevant data are included in Table 2. As shown in Figure 2a, all of the absorption bands are mainly located in the range of 300−400 nm, which could be derived from S_0−S_1 transitions.[49] However, the emission peaks of the boron compounds basically range from 380 to 580 nm, owing to the π-electron delocalization of B^{3-}, which are symmetric as mirror images of the absorption spectra.[50] In addition, compounds **1**−**5** exhibit large Stokes shifts of 103, 95, 86, 83, and 76 nm, respectively, indicating that the as-prepared boron compounds possess the advantage of a relatively wide adjustable range of fluorescence color. It is obvious that the absorption and emission spectra of compounds **1** and **3**−**5** assume a red shift in comparison to that of compound **2**, which is due to the push−pull character effect.[51,52] This can be explained as follows: the electron-withdrawing (F, Cl, or Br) and -donating (CH_3) groups attached on the benzene groups of boron compounds could result in a bathochromic shift by decreasing the electron transition energy and enlarging the conjugation effect, separately. Meanwhile, the steric hindrance of the electron donor methyl could effectively inhibit the close stacking of molecules, thus preventing spectrum broadening, which contributes to the largest red shift of compound **1**.[50] In addition, compound **1** displays the highest absorption and emission intensities, as well as the largest quantum yield (φ_f = 0.63), which are due to the fact that methyl could donate electrons to the conjugated system and therefore increase the amount of transition electrons.[53,54] In contrast, compounds **4** and **5** show a relatively lower intensity in both absorption and emission spectra in comparison to compound **2** due to their electron-withdrawing character. Inconsistent with this effect, the fluorescence spectral intensity of compound **3** is higher than that of compound **2** even though fluorine is an electron-withdrawing group. This is probably caused by the fact that fluorine with a small van der Waals radius can easily form a strong emissive fluorescence state (F^{2-}) to enhance the fluorescence intensity. This also explains why the φ_f value of compound **3** (0.31) is larger than that of compound **2** (0.17).[55]

It is intriguing that all of the boron compounds exhibit intense fluorescence in the solid state (Table 2 and Figure 2b), while their optoelectronic properties are greatly influenced by the nature of the substituents. Similarly to the solution behavior (in MeOH), the emission is red-shifted when an electron-donating (CH_3) or electron-withdrawing (F, Cl, or Br) group is incorporated in the benzene group, in comparison to the unsubstituted fluorophore compound **2**. Surprisingly, the solid-state emission of every boron compound is located at a more red shifted wavelength in comparison to the emission obtained in MeOH (Table 2). According to earlier reports, the reason for this phenomenon can possibly be ascribed to the following aspects: (1) the process of solution equilibrium decreases the ground state energy level of solute molecules and (2) the larger molecular interaction in solid state in comparison to that in the liquid state increases the π-conjugation length.[4] This result also indicates that the variation of solution system (e.g., type, concentration) possibly has a great influence on the fluorescence properties of as-synthesized boron compounds.[56]

To further verify the influence of the solution system on the fluorescence properties of boron compounds, we measured the absorption and emission spectra of compound **1** in different solution systems. First, the optoelectronic properties of compound **1** depend on the solvent, as shown in Figure 2c. A significant shift in the emission wavelength was observed when the solvent was changed among CYH (cyclohexane), TL (toluene), THF (tetrahydrofuran), AN (acetonitrile), and MeOH (methanol), and the detailed optical properties of compound **1** in different solvents are given in Table S6 in the Supporting Information. Specifically, the degree of red shift in the emission spectra of compound **1** deepens when the polarity of the solvent increases. For example, the maximum emission of compound **1** red-shifts from 429 nm in CYH to 471 nm in MeOH. However, the variation of solvent polarity produces a negligible shift in the absorption spectrum in comparison to the emission spectrum, indicating that the dipole moment of the excited state is higher than that of the ground state, which contributes to the larger Stokes shift.[57] Furthermore, the effect of solution concentration on the fluorescence properties of

DOI: 10.1021/acs.organomet.7b00435
Organometallics XXXX, XXX, XXX−XXX

Scheme 3. Mechanism for the Formation of Boron Compounds

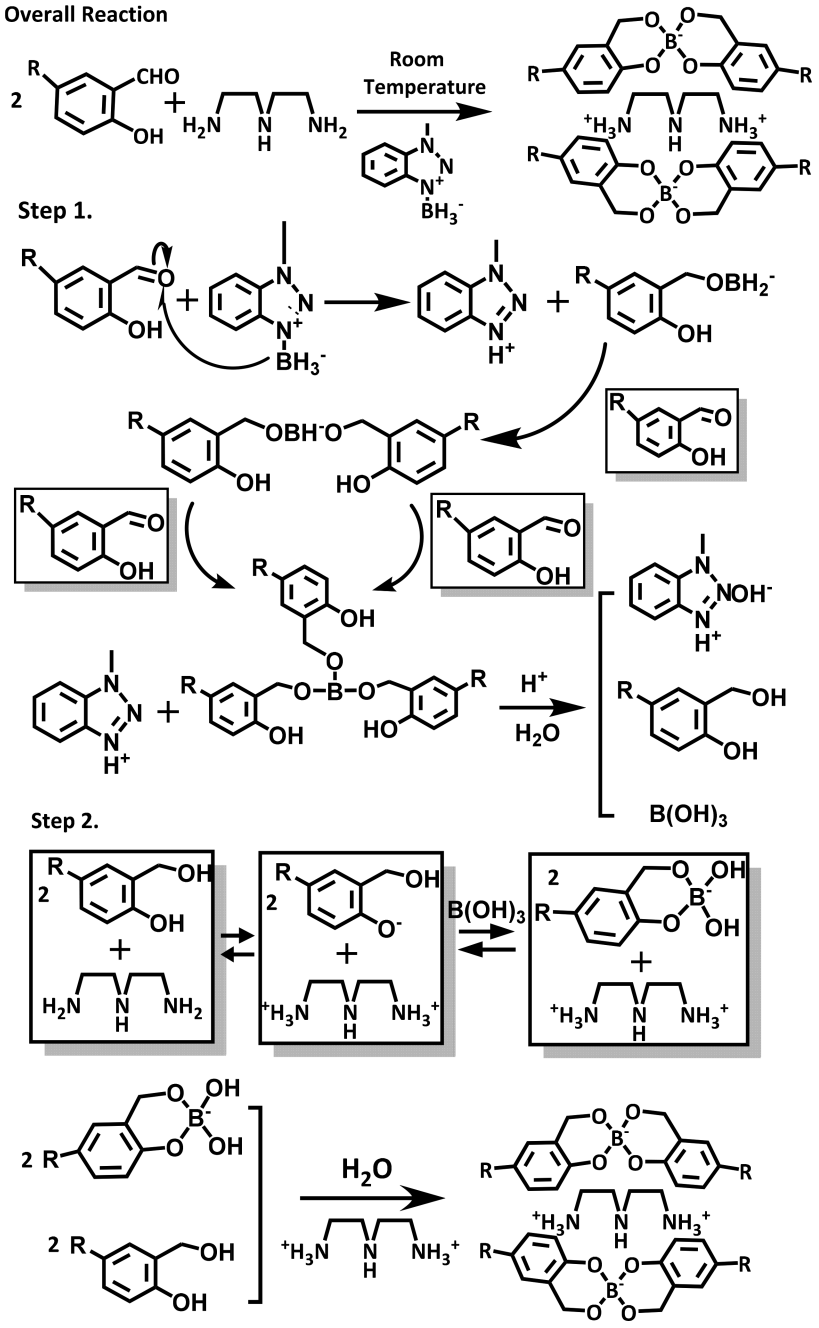

Table 2. Optical Properties of Compounds 1−5

	in methanol					solid state	
compound	λ_{max} (nm) (log ε_{max})[a]	F_{max} (nm)	Stokes shift (nm)	quantum yield Φ[b]	τ (ns)	ex_{max} (nm)	em_{max} (nm)
1	368 (3.96)	471	103	0.63	4.05	375	498
2	330 (3.85)	425	95	0.17	2.55	375	431
3	363 (3.78)	449	86	0.31	2.88	375	468
4	352 (3.56)	435	83	0.09	2.01	375	459
5	348 (3.42)	424	76	0.10	1.07	375	443

[a]Molar absorption (log ε_{max} ±0.1). [b]The fluorescence quantum yield was measured with a concentration of 5×10^{-6} mol/L in MeOH by using perylene (QY = 0.71 in toluene) as the standard.[61,62] The Φ values were corrected for differences in refractive index between the solvents used for sample and reference measurements.

compound **1** was also investigated. Figure 2d illustrates the fluorescence emission spectra of compound **1** with different concentrations in MeOH. It is obvious that the emission peak displays a red shift when the concentration increases, with the

DOI: 10.1021/acs.organomet.7b00435
Organometallics XXXX, XXX, XXX−XXX

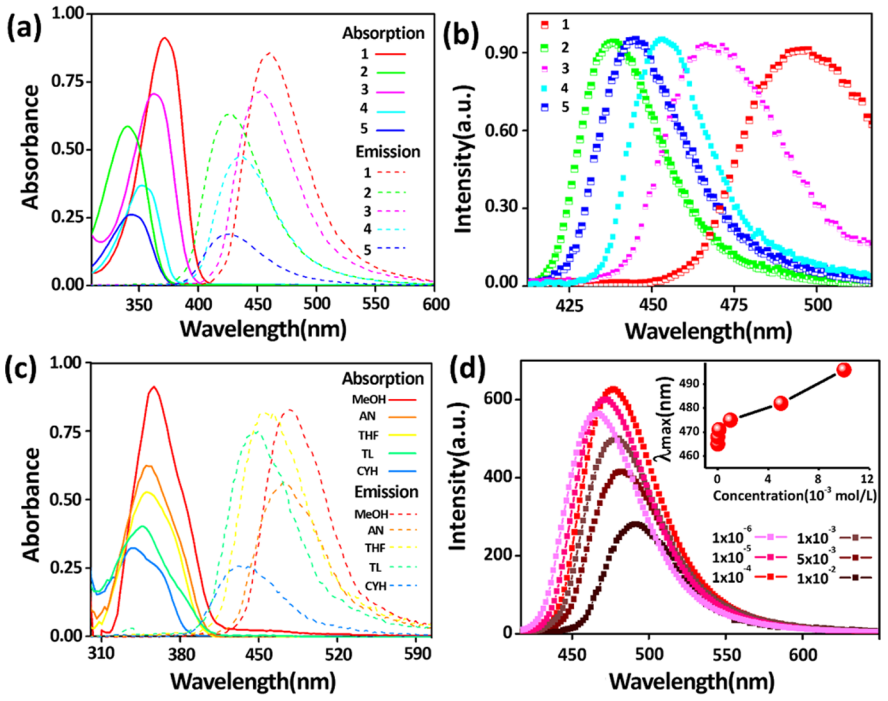

Figure 2. Absorption and florescence emission spectra of compounds **1**−**5** (a) in MeOH solution (1×10^{-4} mol/L) and (b) in the solid state. (c) Spectroscopic properties of compound **1** in MeOH, AN, THF, TL, and CYH (1×10^{-4} mol/L). (d) Fluorescence emission spectra of compound **1** with different concentrations in MeOH (inset: the linear curve of concentration and maximum emission wavelength).

maximum emission shifting from 465 nm ($C_{MeOH} = 1 \times 10^{-6}$ mol/L) to 491 nm ($C_{MeOH} = 1 \times 10^{-2}$ mol/L). From the linear relationship between the concentration and the fluorescence emission (inset of Figure 2d), it can be seen clearly that the emission peak red-shifted gradually with an increase in the concentration. The reason is that boron-containing fluorophores are known to form excimers in concentrated solution and in the solid state, and their emitting properties are greatly influenced by the intermolecular interactions present in the crystal structure.[58−60]

The fluorescence microscopy images of boron compound crystals are shown in Figure 3a−e. We can easily find that all of these crystals display blue luminescence upon the excitation wavelength of 360 nm, which is consistent with the result of fluorescence spectra (both in the liquid state and in the solid state). Furthermore, the fluorescent crystals present different shapes, with rectangles for compound **1**, hexagons for compound **2**, and octagons for compounds **3**−**5**. This is caused by the difference in bond lengths and angles in different boron crystal structures, which affects the orientation of crystal growth.

In addition, we also performed time-resolved fluorescence spectroscopy to estimate the fluorescence lifetime of the five boron compounds. As depicted in Figure 3f−j, the obtained compounds show the signal of decay profiles with an adequately fitted double-exponential decay curve, and their average fluorescence lifetimes (τ) are in the range of 1.07−4.05 ns. Importantly, the methyl-substituted boron compound possesses the longest average fluorescence lifetime, indicating that it has the best fluorescence properties, which is consistent with the result of absorption and emission spectra. For the halogen-substituted boron compounds, the fluorescence lifetime is shortened with the increase in the atomic mass, which is due to the halogen effect.[54]

Finally, temperature- and pH-dependent fluorescence properties were investigated in MeOH. Figure 4a exhibits the emission spectra of compound **1** recorded in the temperature ranging from 193 to 293 K. Obviously, the intensity of fluorescence becomes stronger on cooling, especially when the temperature approaches the freezing point of the solvent. In addition, over the same temperature range, the peak shifts sharply toward higher energy. This situation is consistent with freezing of the solvent, leading to a significant decrease in the magnitude of solvent polarity, which is due to the precipitous change in the dielectric constant as the density of the solvent increases.[63,64] The effect of pH on the fluorescence properties of compound **1** is shown in Figure 4b, which implies that the emission spectrum is slightly influenced by the variation of pH. Both peracid and perbasic treatments could slightly diminish the fluorescence, possibly due to the fact that the boron compounds are unstable under peracid or perbasic conditions.

3.4. Antibacterial Activities. The multifunctional character of the obtained boron compounds was demonstrated by antibacterial experiments. To comprehensively understand the antibacterial activities of as-prepared boron compounds, both Gram-positive (*S. aureus* and *B. subtilis*) and Gram-negative (*E. coli* and *P. aeruginosa*) bacteria were selected as research targets. Control experiments were conducted in the absence of compounds. The inhibition zones of boron compounds with different substituents toward *S. aureus*, *B. subtilis*, *E. coli*, and *P. aeruginosa* are shown in Figure 5 (diameters of inhibition zones are given in Table S7 in the Supporting Information). It is found that the diameters of inhibition zones over different compounds varies with the substituent. For instance, the diameters of the inhibition zone for compounds **1**−**5** against *S. aureus* were 12.4, 11.6, 10.8, 15.2, and 13.2 mm, respectively. Moreover, the sizes of inhibition zones over compounds **1**−**5** against Gram-positive *S. aureus* and *B. subtilis* are evidently larger than those of Gram-negative *E. coli* and *P. aeruginosa*,

DOI: 10.1021/acs.organomet.7b00435
Organometallics XXXX, XXX, XXX−XXX

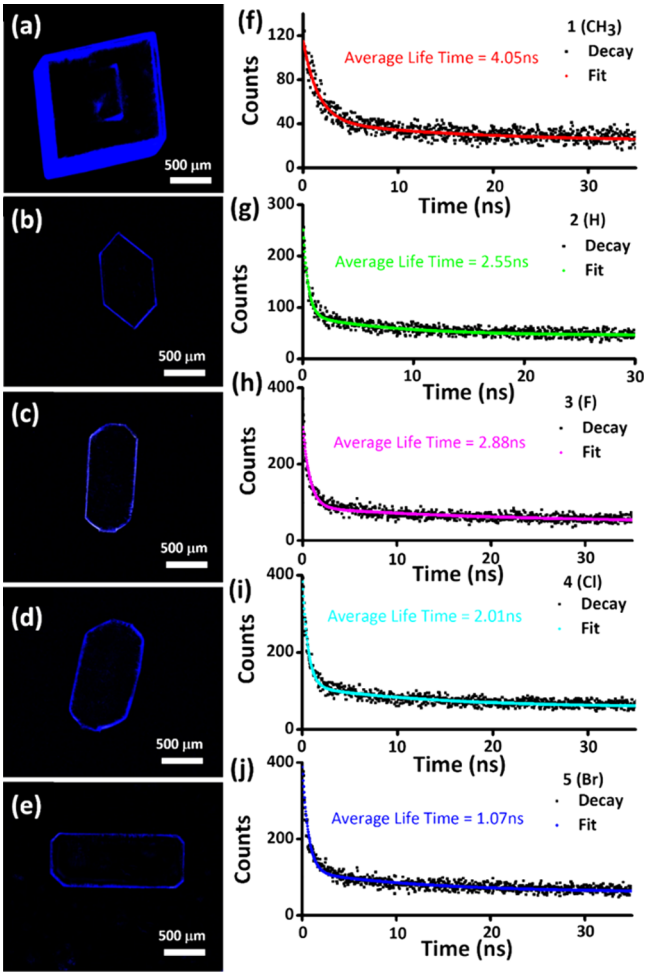

Figure 3. (a–e) Fluorescence microscopy images (at the excitation wavelength of 360 nm) and (f–j) fluorescence decay of crystals of **1**–**5** obtained by diffusing at room temperature.

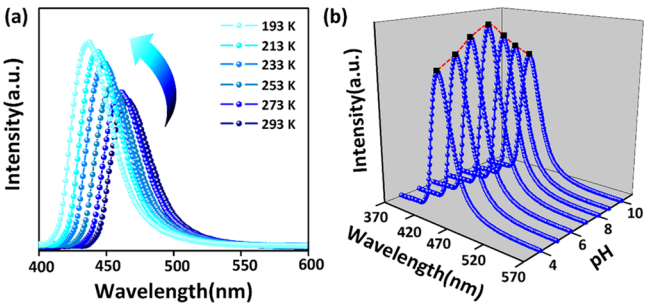

Figure 4. Effects of the (a) temperature and (b) pH on the emission spectrum recorded for compound **1** in MeOH solution (1×10^{-4} mol/L).

which demonstrates that all of the boron compounds exhibit selective antibacterial activities. Remarkably, all compounds strongly inhibit *S. aureus*, *B. subtilis* and *E. coli*, whereas no compounds show obvious antibacterial activity against *P. aeruginosa*. In addition, we can easily find that the inhibition zone diameters of compound **4** (Cl-substituted) are larger than those of other compounds in all antibacterial experiments, indicating that it has the best antibacterial performance.

From the results of the inhibition zone experiments, the as-prepared boron compounds exhibited obvious antibacterial activities toward *S. aureus*, *B. subtilis*, and *E. coli*. Thus, we

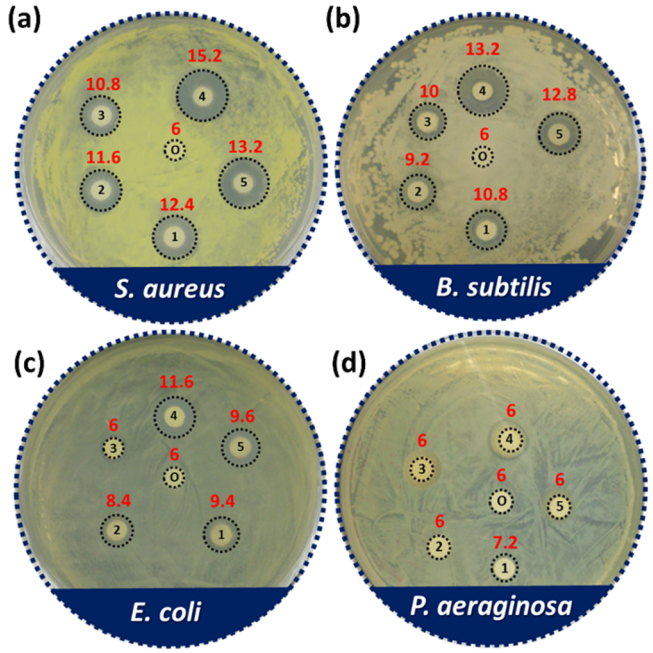

Figure 5. Typical inhibition zones of obtained boron compounds against (a) *S. aureus*, (b) *B. subtilis*, (c) *E. coli*, and (d) *P. aeruginosa* (5 μg/mL, 10 μL). Note that (0) is the blank control in each disk.

selected Gram-positive *S. aureus* and Gram-negative *E. coli* to further examine the antimicrobial activities of boron compounds **1** (CH_3), **2** (H), and **4** (Cl) through their corresponding minimum inhibitory concentration (MIC) and minimum bactericidal concentration (MBC) values. The growth inhibition curves of *S. aureus* and *E. coli* over compounds **1**, **2**, and **4** at different concentrations are shown in Figure 6. When there is no antibacterial agent in the system, the bacteria rapidly breed and reach the maximum peak after 6.5 h for *S. aureus* or 6 h for *E. coli*. After the boron compound is introduced, the reproduction of the bacteria is restrained, and the reproduction ability of the bacteria is negatively correlated to the concentration of the boron compounds. For instance, compound **4** could completely inhibit the *S. aureus* growth at a concentration of 0.25 μg/mL, whereas it only delayed less than 40% of the exponential phase at a concentration of 0.125 μg/mL. The MIC and MBC values for all compounds are shown in Table 3. It is observed that the MIC and MBC values of boron compounds **1**, **2**, and **4** toward the two bacteria varies with their substituents. Specifically, compound **4** with a chlorine substituent possesses the lowest MIC and MBC values, indicating that it has the best antibacterial performance, which is even equivalent in *S. aureus* inhibition to that of commercial antibiotics (the fluoroquinolone derivative ciprofloxacin).[65] On the other hand, the above experiments indicate that the as-prepared boron compounds possess excellent antibacterial properties against both Gram-positive bacteria and Gram-negative bacteria and the antibacterial effect of the boron compounds against the Gram-positive bacteria *S. aureus* is better than that against the Gram-negative bacteria *E. coli*. For example, compound **2** shows an MIC value of 2.0 μg/mL against *S. aureus*, while this value s 16 μg/mL toward *E. coli*. This is probably due to a special cell structure named lipopolysaccharide that only exists in the outer membrane of Gram-negative bacteria, which was reported to provide an effective resistive barrier against boron compounds.[66]

DOI: 10.1021/acs.organomet.7b00435
Organometallics XXXX, XXX, XXX–XXX

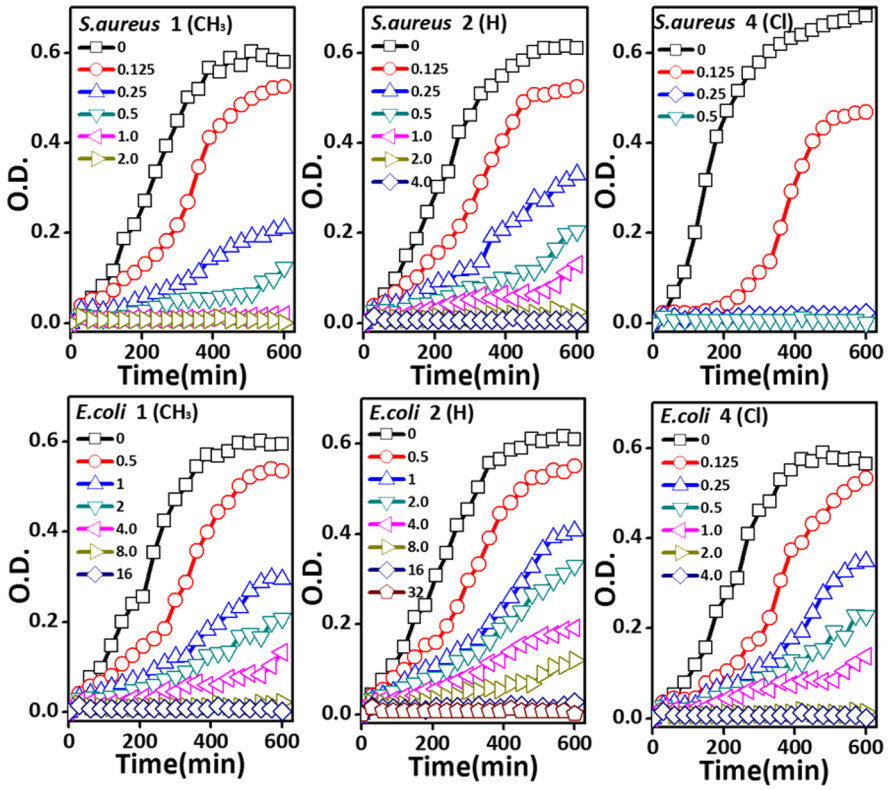

Figure 6. Time-dependent growth curve of different bacteria in the presence of compounds **1** (CH_3), **2** (H), and **4** (Cl).

Table 3. MIC and MBC Values of Compounds 1, 2, and 4 against *S. aureus* and *E. coli*

	S. aureus		*E. coli*	
compound	MIC[a] (μg/mL)	MBC[b] (μg/mL)	MIC (μg/mL)	MBC (μg/mL)
1	1.0	4.0	8.0	64
2	2.0	16	16	128
4	0.25	0.5	2.0	32
ciprofloxacin[c]	0.25	0.5	0.5	1.0

[a]MIC: minimum inhibitory concentration. [b]MBC: minimum bactericidal concentration. [c]Ciprofloxacin: a commercial antibiotic was used as a standard drug.

In addition, the antibacterial sensitivity of the obtained boron compounds against two Gram-positive bacteria (*S. aureus* and *B. subtilis*) was also investigated. Here we performed the colony counting test of compounds **1** (CH_3), **2** (H), and **4** (Cl) against the mixed cultures *S. aureus* and *B. subtilis* in the same agar plate. Control experiments were conducted in the absence of compounds, and the experiments were performed in triplicate. Figure 7 displays the inhibition rates of compounds **1**, **2**, and **4** against the cocultured bacteria. Under the same culture conditions, the inhibition rate of compounds **1**, **2**, and **4** against *S. aureus* is higher than that against *B. subtilis*. For example, when the sample concentration is 0.125 μg/mL, the inhibition rates for compounds **1**, **2**, and **4** are 49.2%, 40.2%, and 65.1% against *S. aureus*, while they are 40.5%, 35.5%, and 51.2% against *B. subtilis*, respectively. With an increase in concentration to 0.5 μg/mL, the inhibition rates increase to 85.2%, 71.2%, and 100% against *S. aureus*, while those against *B. subtilis* are only 78.1%, 62.5%, and 82.2%, respectively. Definitely, *S. aureus* could be completely inhibited with concentrations of 4.0, 16, and 0.5 μg/mL over compounds **1**, **2**, and **4**, respectively. However, *B. subtilis* could be completely inhibited over compounds **1**, **2**, and **4** when the concentrations reach 8.0, 16, and 2.0 μg/mL, respectively. These results further

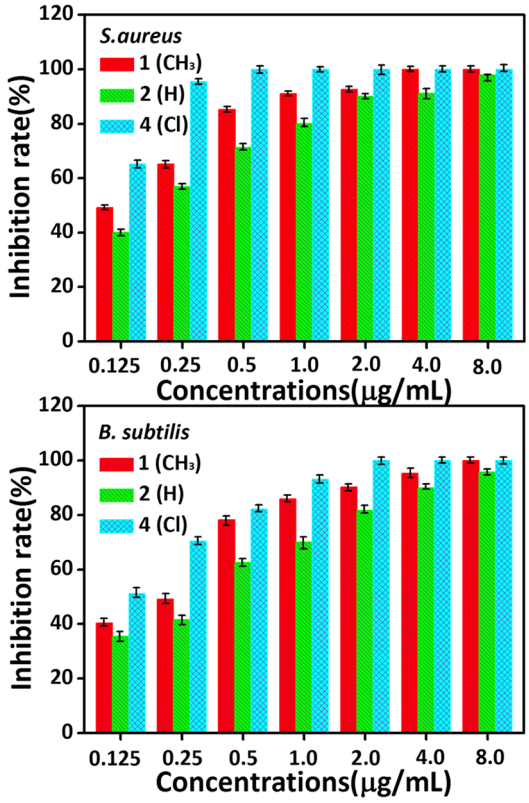

Figure 7. Inhibition rates of compounds **1** (CH_3), **2** (H), and **4** (Cl) against cultured bacterias (*S. aureus*, *B. subtilis*).

DOI: 10.1021/acs.organomet.7b00435
Organometallics XXXX, XXX, XXX−XXX

verify that the boron compounds are more sensitive to *S. aureus* than to *B. subtilis*.

To further prove the bacteria-dependent antibacterial activity, it is necessary to investigate the bacterial cell decomposition. Thus, the leakages of reducing sugars as a measure of cell disruption after treatment with boron compounds **1** (CH_3), **2** (H), and **4** (Cl) were estimated. Figure 8 reveals that an appreciable amount of reducing sugar

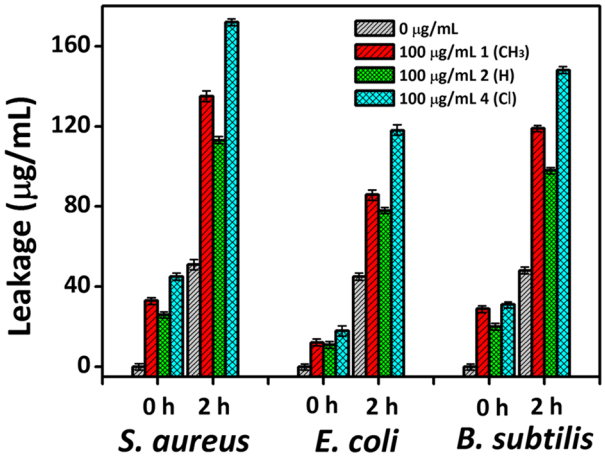

Figure 8. Leakage of reducing sugars from bacteria cells (*S. aureus*, *E. coli*, and *B. subtilis*) treated with compounds **1** (CH_3), **2** (H), and **4** (Cl).

leakage was found in all cases after the boron compound was introduced in comparison to the control experiment, indicating that the obtained reducing sugars must have released due to the decomposition of the bacterial membrane. Furthermore, the leakage amount of reducing sugars varies with the substituents and the kinds of bacteria. For example, after 2 h treatment with compounds **1**, **2**, and **4**, the leakage amounts of reducing sugars in *S. aureus* increase from 33, 26, and 45 μg/mL to 135, 113, and 172 μg/mL, respectively. However, this value increases from 12, 11, and 18 μg/mL to 86, 78, and 118 μg/mL in the case of *E. coli* and from 29, 20, and 31 μg/mL to 119, 98, and 148 μg/mL in the case of *B. subtilis*, respectively. This result implies that compounds **1**, **2**, and **4** could destroy the structure of the membrane and facilitate the leakage of reducing sugars from bacterial cytoplasm. In addition, the leakage amount of reducing sugars of *S. aureus* is higher than that of *B. subtilis* and *E. coli* in all cases, indicating a more severe destruction to the cell membrane of *S. aureus*. Among the three boron compounds, compound **4** causes the largest leakage amount of reducing sugars toward both of the bacteria, demonstrating that it has the best antibacterial ability, which is in accordance with the result of antibacterial experiments.

It is important to understand the reason the obtained boron compounds exhibit different antibacterial activity; thus, the influence of the substituents on the physicochemical properties that are related to the antibacterial activity of boron compounds was then investigated. According to earlier reports, hydrophobicity was highly related to the ability to diffuse through the biological membranes and reach reaction sites, which could directly affect the antimicrobial activity.[67] Therefore, we first utilized the contact angle to characterize the hydrophobic properties of compounds **1**, **2**, and **4**. As shown in Figure 9a–c, the contact angles of compounds **1**, **2** and **4** are 58.8, 45.8, and 66.6°, respectively, indicating that compounds **1** (CH_3) and **4**

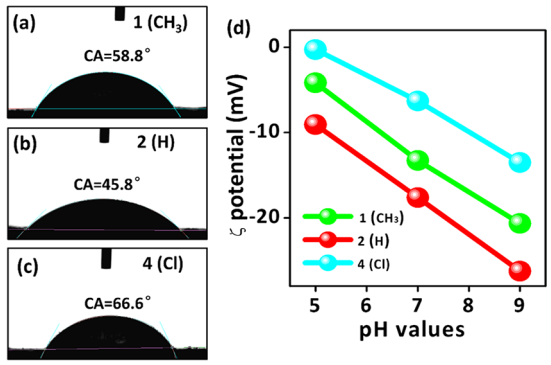

Figure 9. (a–c) Contact angles and (d) ζ potentials of compounds **1**, **2**, and **4**.

(H) both show superior hydrophobic character in comparison to unsubstituted compound **2**. Interestingly, the incorporation of a hydrophobic substituent (chlorine) could improve the hydrophobicity of boron compounds, thus leading to compound **4** having the best hydrophobic properties.

Moreover, an understanding of the electric charge on the surface of boron compounds deserves further investigation in order to clarify the electrostatic interaction between bacteria and compounds, which greatly influences the absorption process and thus causing differences in the inactivation process. ζ potential analysis was therefore performed in LB liquid medium with different pH values. As presented in Figure 9d, the surfaces of compounds **1**, **2**, and **4** are all negatively charged in LB liquid medium with pHs ranging from 5 to 9. Because the bacteria are also negatively charged in LB liquid, the boron compounds and bacteria would repel each other in the LB liquid medium in the antibacterial experiments (pH 7). However, the boron compound **4** with a chlorine substituent (−6.3 mV) is less negatively charged than compounds **1** and **2** (−13.3 and −17.6 mV), indicating a weaker repulsive force between compound **4** and bacteria and thus a better absorption of bacteria, which contributes to its better antibacterial activity.

4. CONCLUSION

In conclusion, we developed a facile strategy to synthesize a series of multifunctional boron compounds. Our synthetic strategy has allowed us to prepare boron compounds containing different types of substituents (CH_3, F, Cl, and Br) on each benzene ring of salicylic aldehyde, which to the best of our knowledge is not known in the literature. These boron compounds exhibit substituent-dependent fluorescence properties that are highly related to the electron-withdrawing and electron-donating abilities of the substituent. Interestingly, the methyl-substituted boron compound exhibited bright fluorescence in both the liquid and solid state with high quantum yields, large Stokes shifts, and long lifetimes, indicating its potential applications in solid-state emitting materials. In addition, the influence of different factors on the fluorescence properties of boron compounds, including solvent (i.e., polarity, concentration), temperature, and pH, was also discussed in detail. In addition, the as-synthesized boron compounds also exhibited efficient bacterium-selective and substituent-dependent antibacterial activities. The chlorine-substituted boron compound even possessed antibacterial activity comparable with that of commercial antibiotics. The contact angle characterization and ζ potential analysis further proved that the difference in hydrophobic properties and

DOI: 10.1021/acs.organomet.7b00435
Organometallics XXXX, XXX, XXX−XXX

charging on the surface contributes to the diversity in antibacterial activity of boron compounds. This work provides a new strategy for the design of multifunctional organoboron compounds and the mediation of their properties.

■ ASSOCIATED CONTENT

Supporting Information

The Supporting Information is available free of charge on the ACS Publications website at DOI: 10.1021/acs.organomet.7b00435.

Elemental analyses, NMR spectral data, FT-IR, crystal structure data of boron compounds, molecular structure and structural descriptions of compounds **1** and **3**−**5**, photoluminescence in different solvents, and sizes of inhibition zones of compounds (PDF)

Accession Codes

CCDC 1534451−1534455 contain the supplementary crystallographic data for this paper. These data can be obtained free of charge via www.ccdc.cam.ac.uk/data_request/cif, or by emailing data_request@ccdc.cam.ac.uk, or by contacting The Cambridge Crystallographic Data Centre, 12 Union Road, Cambridge CB2 1EZ, UK; fax: +44 1223 336033.

■ AUTHOR INFORMATION

Corresponding Author

*Hong Zhou Tel: (+86)13871359786 E-mail: hzhouh@126.com.

ORCID

Hong Zhou: 0000-0003-2409-784X

Notes

The authors declare no competing financial interest.

■ ACKNOWLEDGMENTS

We are grateful for financial support from the Natural Science Foundation of China (21171135), the eighth postgraduate education innovation fund of Wuhan Institute of Technology, China (CX2016174), and the support of ^{1}H NMR and ^{13}C NMR spectra from the Shiyanjia laboratory.

■ REFERENCES

(1) Erten-Ela, S.; Yilmaz, M. D.; Icli, B.; Dede, Y.; Icli, S.; Akkaya, E. U. *Org. Lett.* **2008**, *10*, 3299−3302.
(2) Kim, T. I.; Park, J.; Park, S.; Choi, Y.; Kim, Y. *Chem. Commun.* **2011**, *47*, 12640−12642.
(3) Loudet, A.; Burgess, K. *Chem. Rev.* **2007**, *107*, 4891−4932.
(4) Shimizu, M.; Hiyama, T. *Chem. - Asian J.* **2010**, *5*, 1516−1531.
(5) Zhou, Y.; Kim, J. W.; Nandhakumar, R.; Kim, M. J.; Cho, E.; Kim, Y. S.; Jang, Y. H.; Lee, C.; Han, S.; Kim, K. M.; Kim, J. J.; Yoon, J. *Chem. Commun.* **2010**, *46*, 6512−6514.
(6) Banal, J. L.; Zhang, B. L.; Jones, D. J.; Ghiggino, K. P.; Wong, W. W. H. *Acc. Chem. Res.* **2017**, *50*, 49−57.
(7) Li, D.; Zhang, H. Y.; Wang, Y. *Chem. Soc. Rev.* **2013**, *42*, 8416−8433.
(8) Lodeiro, C.; Pina, F. *Coord. Chem. Rev.* **2009**, *253*, 1353−1383.
(9) Ma, D. L.; Chan, D. S. H.; Leung, C. H. *Acc. Chem. Res.* **2014**, *47*, 3614−3631.
(10) Paun, A.; Hadade, N. D.; Paraschivescu, C. C.; Matache, M. *J. Mater. Chem. C* **2016**, *4*, 8596−8610.
(11) Zhao, J. Z.; Wu, W. H.; Sun, J. F.; Guo, S. *Chem. Soc. Rev.* **2013**, *42*, 5323−5351.
(12) Hong, Y. N.; Lam, J. W. Y.; Tang, B. Z. *Chem. Commun.* **2009**, 4332−4353.
(13) Massin, J.; Dayoub, W.; Mulatier, J. C.; Aronica, C.; Bretonniere, Y.; Andraud, C. *Chem. Mater.* **2011**, *23*, 862−873.
(14) Guo, B.; Cai, X. L.; Xu, S. D.; Fateminia, S. M. A.; Liu, J.; Liang, J.; Feng, G. X.; Wu, W. B.; Liu, B. *J. Mater. Chem. B* **2016**, *4*, 4690−4695.
(15) Huang, M. N.; Yu, R. N.; Xu, K.; Ye, S. X.; Kuang, S.; Zhu, X. H.; Wan, Y. Q. *Chem. Sci.* **2016**, *7*, 4485−4491.
(16) D'aleo, A.; Felouat, A.; Heresanu, V.; Ranguis, A.; Chaudanson, D.; Karapetyan, A.; Giorgi, M.; Fages, F. *J. Mater. Chem. C* **2014**, *2*, 5208−5215.
(17) Kubota, Y.; Tsuzuki, T.; Funabiki, K.; Ebihara, M.; Matsui, M. *Org. Lett.* **2010**, *12*, 4010−4013.
(18) Kumar, G. R.; Thilagar, P. *Dalton Trans.* **2014**, *43*, 3871−3879.
(19) Poon, C. T.; Lam, W. H.; Yam, V. W. W. *Chem. - Eur. J.* **2013**, *19*, 3467−3476.
(20) Xu, S. P.; Evans, R. E.; Liu, T. D.; Zhang, G. Q.; Demas, J. N.; Trindle, C. O.; Fraser, C. L. *Inorg. Chem.* **2013**, *52*, 3597−3610.
(21) Park, S. H.; Ahn, D. *IEEE Photonics Technol. Lett.* **2017**, *29*, 1042−1045.
(22) Perras, F. A.; Bryce, D. L. *Chem. Sci.* **2014**, *5*, 2428−2437.
(23) Wu, T. L.; Yeh, C. H.; Hsiao, W. T.; Huang, P. Y.; Huang, M. J.; Chiang, Y. H.; Cheng, C. H.; Liu, R. S.; Chiu, P. W. *ACS Appl. Mater. Interfaces* **2017**, *9*, 14998−15004.
(24) Zhang, X. F.; Xiao, Y.; Qi, J.; Qu, J. L.; Kim, B.; Yue, X. L.; Belfield, K. D. *J. Org. Chem.* **2013**, *78*, 9153−9160.
(25) Ozdemir, T.; Bila, J. L.; Sozmen, F.; Yildirim, L. T.; Akkaya, E. U. *Org. Lett.* **2016**, *18*, 4821−4823.
(26) Ono, K.; Yoshikawa, K.; Tsuji, Y.; Yamaguchi, H.; Uozumi, R.; Tomura, M.; Taga, K.; Saito, K. *Tetrahedron* **2007**, *63*, 9354−9358.
(27) Nielsen, F. H. *Nutr. Rev.* **2008**, *66*, 183−191.
(28) Woods, W. G. *Environ. Health Persp.* **1994**, *102*, 5−11.
(29) Galer, P.; Korosec, R. C.; Vidmar, M.; Sket, B. *J. Am. Chem. Soc.* **2014**, *136*, 7383−7394.
(30) Zhou, Y.; Chen, Y. Z.; Cao, J. H.; Yang, Q. Z.; Wu, L. Z.; Tung, C. H.; Wu, D. Y. *Dyes Pigm.* **2015**, *112*, 162−169.
(31) Dias, L. C.; Polo, E. C.; Ferreira, M.a.B.; Tormena, C. F. *J. Org. Chem.* **2012**, *77*, 3766−3792.
(32) Rubinstein, N.; Liu, P.; Miller, E. W.; Weinstain, R. *Chem. Commun.* **2015**, *51*, 6369−6372.
(33) Lacina, K.; Skladal, P. *Electrochim. Acta* **2011**, *56*, 10246−10252.
(34) Takahashi, S.; Abiko, N.; Haraguchi, N.; Fujita, H.; Seki, E.; Ono, T.; Yoshida, K.; Anzai, J. *J. Environ. Sci.* **2011**, *23*, 1027−1032.
(35) Marepally, S. R.; Yao, M. L.; Kabalka, G. W. *Future Med. Chem.* **2013**, *5*, 693−704.
(36) Baker, S. J.; Tomsho, J. W.; Benkovic, S. J. *Chem. Soc. Rev.* **2011**, *40*, 4279−4285.
(37) Vogels, C. M.; Westcott, S. A. *Chem. Soc. Rev.* **2011**, *40*, 1446−1458.
(38) Carr, J. M.; Duggan, P. J.; Humphrey, D. G.; Platts, J. A.; Tyndall, E. M. *Aust. J. Chem.* **2005**, *58*, 901−911.
(39) Carr, J. M.; Duggan, P. J.; Humphrey, D. G.; Tyndall, E. M. *Aust. J. Chem.* **2005**, *58*, 21−25.
(40) Carr, J. M.; Duggan, P. J.; Humphrey, D. G.; Platts, J. A.; Tyndall, E. M. *Aust. J. Chem.* **2010**, *63*, 1423−1429.
(41) Pitchumony, T. S.; Spingler, B.; Motterlini, R.; Alberto, R. *Chimia* **2008**, *62*, 277−279.
(42) Forsyth, S. A.; Macfarlane, D. R. *J. Mater. Chem.* **2003**, *13*, 2451−2456.
(43) Liao, W. Y.; Chen, Y. F.; Liu, Y. X.; Duan, H. F.; Petersen, J. L.; Shi, X. D. *Chem. Commun.* **2009**, 6436−6438.
(44) Benner, K.; Klufers, P. *Carbohydr. Res.* **2000**, *327*, 287−292.
(45) Chandrasekhar, S.; Shrinidhi, A. *Synth. Commun.* **2014**, *44*, 2051−2056.
(46) Lin, R. C.; Cheng, J.; Ding, L. K.; Song, W. L.; Zhou, J. H.; Cen, K. F. *Bioresour. Technol.* **2015**, *197*, 323−328.
(47) Song, P.; Ruan, M. B.; Sun, X. J.; Zhang, Y. W.; Xu, W. L. *J. Phys. Chem. B* **2014**, *118*, 10224−10231.

DOI: 10.1021/acs.organomet.7b00435
Organometallics XXXX, XXX, XXX−XXX

(48) Miyazaki, Y.; Matsuo, H.; Fujimori, T.; Takemura, H.; Matsuoka, S.; Okobira, T.; Uezu, K.; Yoshimura, K. *Polyhedron* **2008**, *27*, 2785−2790.
(49) Chinna Ayya, S. P.; Thilagar, P. *Inorg. Chim. Acta* **2014**, *411*, 97−101.
(50) Kumbhar, H. S.; Gadilohar, B. L.; Shankarling, G. S. *Spectrochim. Acta, Part A* **2015**, *146*, 80−87.
(51) Guieu, S.; Pinto, J.; Silva, V. L. M.; Rocha, J.; Silva, A. M. S. *Eur. J. Org. Chem.* **2015**, *2015*, 3423−3426.
(52) Zhang, Z. L.; Edkins, R. M.; Nitsch, J.; Fucke, K.; Eichhorn, A.; Steffen, A.; Wang, Y.; Marder, T. B. *Chem. - Eur. J.* **2015**, *21*, 177−190.
(53) Kubota, Y.; Hara, H.; Tanaka, S.; Funabiki, K.; Matsui, M. *Org. Lett.* **2011**, *13*, 6544−6547.
(54) Lakshmi, V.; Ravikanth, M. *RSC Adv.* **2014**, *4*, 44327−44336.
(55) Feng, X.; Sun, Y. L.; Li, R. F.; Zhang, T.; Guo, N.; Wang, L. Y. *Inorg. Chem. Commun.* **2016**, *73*, 190−195.
(56) Zakerhamidi, M. S.; Ghanadzadeh, A.; Moghadam, M. *Spectrochim. Acta, Part A* **2011**, *79*, 74−81.
(57) Sun, Y.; Liang, X. H.; Zhao, Y. Y.; Fan, J. *Spectrochim. Acta, Part A* **2013**, *102*, 194−199.
(58) Cao, Q.; Xiao, S. Z.; Mao, M. F.; Chen, X. H.; Wang, S.; Li, L.; Zou, K. *J. Organomet. Chem.* **2012**, *717*, 147−151.
(59) Koch, M.; Perumal, K.; Blacque, O.; Garg, J. A.; Saiganesh, R.; Kabilan, S.; Balasubramanian, K. K.; Venkatesan, K. *Angew. Chem., Int. Ed.* **2014**, *53*, 6378−6382.
(60) Vincent, M.; Beabout, E.; Bennett, R.; Hewavitharanage, P. *Tetrahedron Lett.* **2013**, *54*, 2050−2054.
(61) Crosby, G. A.; Demas, J. N. *J. Phys. Chem.* **1971**, *75*, 991−1024.
(62) Olmsted, J. *J. Phys. Chem.* **1979**, *83*, 2581−2584.
(63) Bublitz, G. U.; Boxer, S. G. *J. Am. Chem. Soc.* **1998**, *120*, 3988−3992.
(64) Vath, P.; Zimmt, M. B.; Matyushov, D. V.; Voth, G. A. *J. Phys. Chem. B* **1999**, *103*, 9130−9140.
(65) Semenov, V. E.; Mikhailov, A. S.; Voloshina, A. D.; Kulik, N. V.; Nikitashina, A. D.; Zobov, V. V.; Kharlamov, S. V.; Latypov, S. K.; Reznik, V. S. *Eur. J. Med. Chem.* **2011**, *46*, 4715−4724.
(66) Vilakazi, C. S.; Dubery, I. A.; Piater, L. A. *Plant Physiol. Biochem.* **2017**, *111*, 155−165.
(67) Jorge, S. D.; Masunari, A.; Rangel-Yagui, C. O.; Pasqualoto, K. F. M.; Tavares, L. C. *Bioorg. Med. Chem.* **2009**, *17*, 3028−3036.

DOI: 10.1021/acs.organomet.7b00435
Organometallics XXXX, XXX, XXX−XXX